AFRL-RS-PS-
TP-2021-0004

FULL 3-D SIMULATION AND OPTIMIZATION OF GIGAWATT CLASS C-BAND 20% EFFICIENT COAXIAL VIRCATOR

Bud Denny, Christopher Leach, Jason Hammond

21 January 2021

Technical Paper

AIR FORCE RESEARCH LABORATORY
Directed Energy Directorate
3550 Aberdeen Ave SE
AIR FORCE MATERIEL COMMAND
KIRTLAND AIR FORCE BASE, NM 87117-5776

NOTICE AND SIGNATURE PAGE

Using Government drawings, specifications, or other data included in this document for any purpose other than Government procurement does not in any way obligate the U.S. Government. The fact that the Government formulated or supplied the drawings, specifications, or other data, does not license the holder or any other person or corporation; or convey any rights or permission to manufacture, use, or sell any patented invention that may relate to them.

Qualified requestors may obtain copies of this report from the Defense Technical Information Center (DTIC) (http://www.dtic.mil).

AFRL-RS-PS-TP-2021-0004 HAS BEEN REVIEWED AND IS APPROVED FOR PUBLICATION IN ACCORDANCE WITH ASSIGNED DISTRIBUTION STATEMENT.

DENNY.BUD.A.1522554495 Digitally signed by DENNY.BUD.A.1522554495 Date: 2021.03.18 14:43:01 -06'00'

BUD DENNY
Associate Mathematician
Effects and Modeling

HAZEL.ASHLEY.R.1106465211 Digitally signed by HAZEL.ASHLEY.R.1106465211 Date: 2021.03.18 14:59:12 -06'00'

MAJ ASHLEY HAZEL
Branch Chief
Effects and Modeling

This report is published in the interest of scientific and technical information exchange, and its publication does not constitute the Government's approval or disapproval of its ideas or findings.

REPORT DOCUMENTATION PAGE

Form Approved

OMB No. 0704-0188

1. REPORT DATE *(DD-MM-YYYY)*	2. REPORT TYPE	3. DATES COVERED *(From - To)*
21-01-2021	Technical Paper	10-08-2020 to 28-09-2020

4. TITLE AND SUBTITLE

Full 3-D Simulation and Optimization of Gigawatt Class C-Band 20% Efficient Coaxial Vircator

5a. CONTRACT NUMBER

5b. GRANT NUMBER

5c. PROGRAM ELEMENT NUMBER

6. AUTHOR(S)

Bud Denny, Christopher Leach, Jason Hammond

5d. PROJECT NUMBER

5e. TASK NUMBER

5f. WORK UNIT NUMBER

DOEW

7. PERFORMING ORGANIZATION NAME(S) AND ADDRESS(ES)

Air Force Research Laboratory
High Power Electromagnetic Division
3550 Aberdeen Ave SE
Kirtland AFB, NM 87117-5776

8. PERFORMING ORGANIZATION REPORT NUMBER

9. SPONSORING/MONITORING AGENCY NAME(S) AND ADDRESS(ES)

10. SPONSOR/MONITOR'S ACRONYM(S)

AFRL/RDHE

11. SPONSOR/MONITOR'S REPORT NUMBER(S)

AFRL-RS-PS-TP-2021-0004

12. DISTRIBUTION/AVAILABILITY STATEMENT

Approved for public release; distribution is unlimited. Public Affairs release approval #AFRL-2020-0165.

13. SUPPLEMENTARY NOTES

14. ABSTRACT

An investigation of several configurations of a gigawatt class coaxial triode vircator is presented. To maximize averaged power output efficiency, several device dimensions are optimized. Simulations of the source were carried out using the Improved Concurrent Electromagnetic Particle in Cell (ICEPIC) code. The resulting optimized device has 2.08 GW of output power with a steady state efficiency of 20%. The device's output power is almost purely in the TM_{01} mode. The operating frequency is approximately 4.43 GHz. Additionally presented is a configuration designed to mitigate explosive emission on undesirable surfaces along the cathode. It successfully keeps non-emission surface E-fields below 300 kV/cm while maintaining multi-gigawatt output power.

15. SUBJECT TERMS

HPM; High Power Microwave

16. SECURITY CLASSIFICATION OF:			17. LIMITATION OF ABSTRACT	18. NUMBER OF PAGES	19a. NAME OF RESPONSIBLE PERSON
a. REPORT	b. ABSTRACT	c. THIS PAGE			Bud Denny
UNCLASSIFIED	UNCLASSIFIED	UNCLASSIFIED	SAR	11	19b. TELEPHONE NUMBER *(include area code)* 505-846-2751

Full 3-D Simulation and Optimization of Gigawatt Class C-Band 20% Efficient Coaxial Vircator

Bud Denny, Jason Hammond, Christopher Leach

***Abstract*—An investigation of several configurations of a gigawatt class coaxial triode vircator is presented. To maximize averaged power output efficiency, several device dimensions are optimized. Simulations of the source were carried out using the Improved Concurrent Electromagnetic Particle in Cell (ICEPIC) code. The resulting optimized device has 2.08 GW of output power with a steady state efficiency of 20%. The device's output power is almost purely in the TM_{01} mode. The operating frequency is approximately 4.43 GHz. Additionally presented is a configuration designed to mitigate explosive emission on undesirable surfaces along the cathode. It successfully keeps non-emission surface E-fields below 300 kV/cm while maintaining multi-gigawatt output power.**

***Index Terms*—Coaxial vircator, high-power microwaves (HPM), triode, optimization.**

I. Introduction

Virtual cathode oscillators (vircators) are of research interest because they have gigawatt power output, simple geometries, and potential for tunability. Furthermore, they require no external magnetic field [1], [2]. However, vircators historically suffer from low power-conversion efficiency, typically below 5% [2]. Over the past decade, with the assistance of both theoretical analysis and simulation studies, the efficiency of simulated vircators has been improved to approximately 15%. These more efficient designs include an axial multistage vircator that operates with several virtual cathodes [3], coaxial vircators with a premodulted electron beam [4], [5], and a novel coaxial triode design [6]. Despite these incremental improvements, vircator designs in literature have failed to achieve a 20% power conversion efficiency in the gigawatt range, especially when operating above 4 GHz. In this paper such a source is presented. Furthermore the device operates in a C-band frequency, a band relatively unexplored in the case of vircator. Finally, this paper seeks to provide a procedure of optimization that could increase the power and efficiency of an arbitrary source, particularly those with a simple geometry.

A vircator operates by injecting a high current relativistic beam into a vacuum cavity that exceeds the space charge limited current. The result is a high electron density virtual cathode which oscillates at its plasma frequency. The virtual cathode's oscillations and the electron reflex oscillations generate the device's microwave power output. These details and more are described in [2]. The frequencies of the device are strongly dependent on the anode-cathode gap and diode voltage. Therefore, fixing the anode-cathode gap and diode voltage while adjusting various device dimensions will not change the device's output frequency. This relationship, in the coaxial vircator case, is derived in [7] and [8].

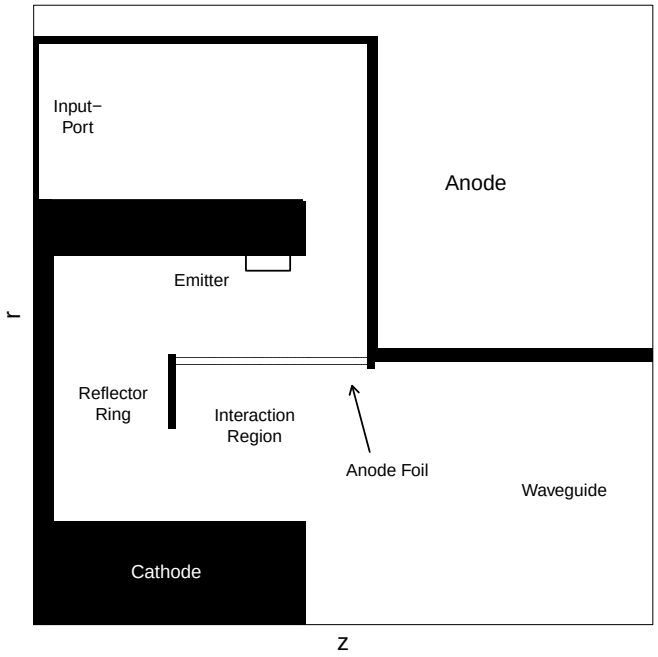

Fig. 1: Schematic of the coaxial triode vircator with reflection cavity.

Improvements by [9] add a reflector ring near the beam interaction region of a coaxial vircator. This can reduce competition of TE modes with the desired TM_{01} mode. The design in [6] applies the ring reflector to a triode design to achieve pure TM_{01} output. The devices proposed and simulated in [6] have an efficiency of 15%

and power outputs of 1.7 GW and 2.2 GW. The device provided here takes the same base design presented in [6]; it's a triode coaxial vircator with a reflector ring. However, the device presented in this paper is C-band and has a power conversion efficiency of 20%. The high efficiency and over 2 GW output power are achieved using a novel optimization until convergence technique. A schematic of the design can be found in Fig. 1.

The optimization is performed using the software ICEPIC and the software Dakota [10]. That is, source simulations are done using the particle-in-cell software ICEPIC [11] run in parallel. The optimizations are carried out with various methods from Sandia National Lab's software Dakota [10].

II. Device Description

The schematic for the triode coaxial vircator with reflection cavity is shown in Fig. 1. An incoming power pulse is introduced at the input port, resulting in a large voltage across the cathode and anode foil. The emitter is a surface on the outer cathode which is primed for electron emission. This is modeled using space charge limited field emission: when the voltage pulse reaches the emitter, a high current electron beam is injected from it into the interaction region. A virtual cathode is then formed in the interaction region producing RF that will propagate through the waveguide where it will be extracted. The physical dimensions of the device and their roles will be expounded in this section.

The difference between a typical coaxial vircator and a triode coaxial vircator is the inner-cathode-rod attached to the main cathode. Its radius is labeled r_c in Fig. 2. The inner-cathode-rod is used to assist electrons in moving between the virtual cathode and real cathode. Furthermore, the inner cathode-rod serves to change the dominant mode in the interaction region from TE_{11} to TEM. The mode competition between the TM_{01} mode and the TE_{11} mode is reduced as a result. The output power is almost exclusively in the TM_{01} mode for a triode design. Further implications of the inner-cathode-rod are highlighted in [6].

The ring reflector whose radial width is labeled h in Fig. 2 also has the purpose of suppressing the the TE_{11} mode in favor of the TM_{01} [9]. The ring reflector further has the purpose of reflecting radiation to enhance the beam-wave interaction [6]. The design in this paper uses the ring reflector to create a resonant cavity in the interaction region. Removing the ring reflector has the ruinous effect of a drastic power output decrease and a reduction of output frequency.

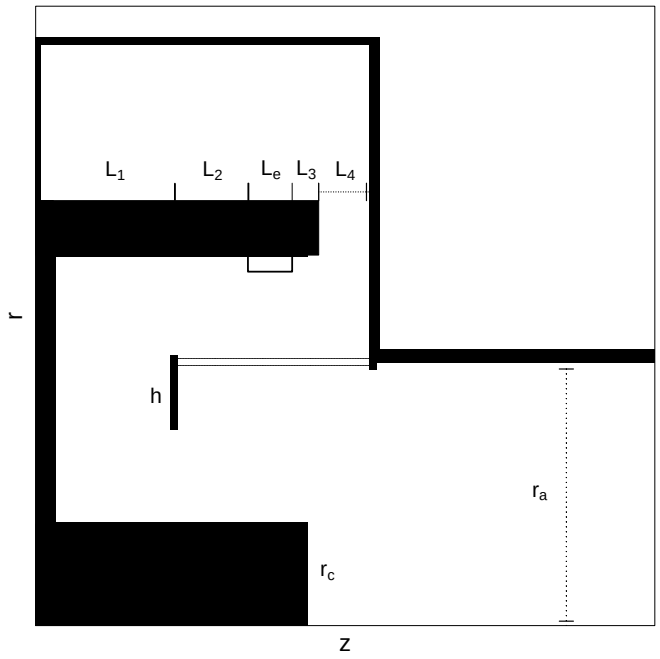

Fig. 2: Schematic of the coaxial triode vircator with physical dimensions labeled. The schematic uses the a similar naming convention as [6].

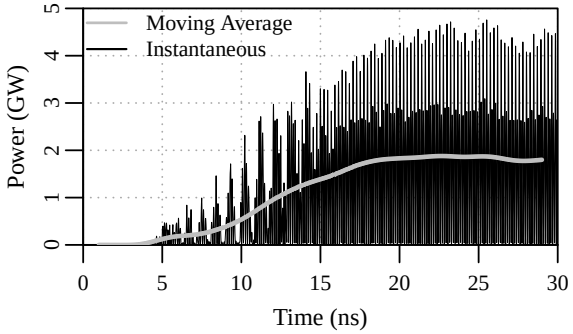

Fig. 3: Output power waveform of coaxial vircator prior to optimization.

The remaining variables in Fig. 2 are present in a typical coaxial vircator. The lengths L_1, L_2, L_e, L_3, L_4, represent, respectively, the z-distances from the cathode to the reflector ring, the reflector ring to the left of the emitter, the emitter length in z, the right of the emitter to the end of the cathode, and the gap right of the cathode to the anode. Finally the radius of the waveguide, which is carved out of the anode, is represented by r_a.

III. Simulations

Simulations of the device presented in this paper are done in 3-D using the massively parallel finite-

difference time domain electromagnetic particle-in-cell code ICEPIC [11]. Simulations are done with a uniform mesh-size of $\Delta x = 0.88$ mm and a conformal method is used at the boundaries [12]. The time step Δt is chosen so that the Courant number is 0.99 i.e. so that $c\ \Delta t/\Delta x = 0.99$.

Mode amplitudes are determined by computing a dot-product of the simulated fields with analytic fields of that mode. Power is measured by integrating the Poynting vector on a surface that cuts the output waveguide: this power is averaged over the final 10 ns (the instantaneous output power from 20 ns to 30 ns) of the simulation to compute a local time-averaged power, which we report as the output power. Voltages are measured via line integral of electric fields. Input current is measured using Ampere's Law just inside the input port. Frequencies are measured by taking the fast Fourier transform of the downstream electric field's z-component. The anode foil is modeled via a thin surface of perfect metal conductor which mostly allows electrons through: each electron has a fixed probability, 0.95 is used unless stated otherwise, of transmission each time it impinges that surface. Given that the operating frequency of the device is about 4.43 GHz, the resolution is about 50 cells per free-space wavelength.

A typical simulation of the coaxial triode vircator goes as follows: A 30 ns input voltage wave is launched into the vircator via the input-port labeled in Fig. 1. The wave has a maximum voltage of about 566 kV and a rise time of 5 ns. The emitter will then begin injecting electrons into the interaction region when the diode voltage exceeds a predetermined threshold of 2 kV/cm. The injected beam will typically reach a steady state current of 18 kA. A virtual cathode is formed in the interaction region producing the RF for the device. The output power is then measured in the waveguide approximately 28 cm downstream before being absorbed in a PML (perfectly matched layer). The impedance of the tube will be about 30 Ω.

The dimensions of the device prior to optimization, in centimeters, are $L_1 = 5.44,\ L_2 = 2.08,\ L_e = 3.20,\ L_3 = 0.64,\ L_4 = 3.08,\ r_a = 4.70,\ r_c = 1.83,\ h = 1.20$. The device has an anode-cathode gap, the radial distance from the anode foil to the emitter, of 2.87 cm with a voltage of 545 kV across it. Simulations for this device yield a steady state power output of 1.84 GW with an efficiency of 16.6% operating at a frequency of 4.39 GHz. The output power mode is 98% in the TM_{01}.

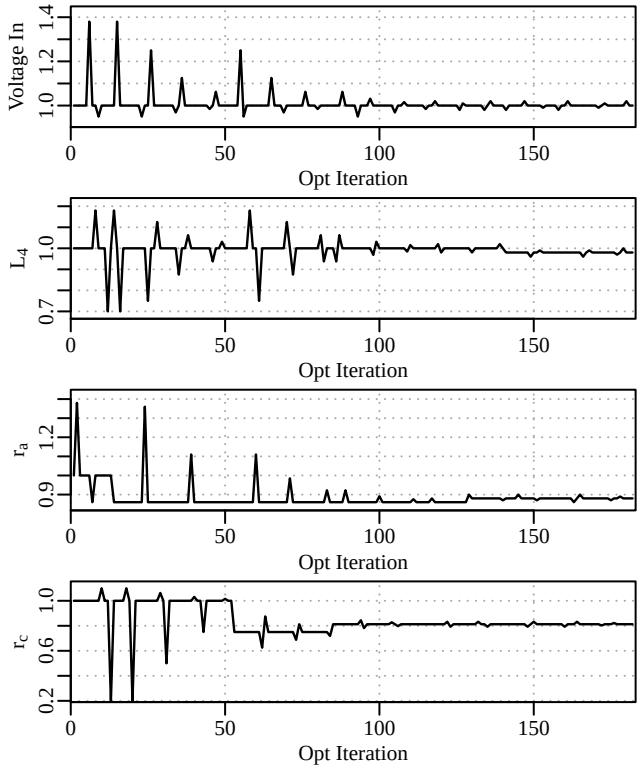

Fig. 4: Plots of optimization iterations converging for various variable scales.

IV. Optimization of Device Dimensions

In view of the low efficiency of vircators, an optimization with an objective of maximum efficiency is performed. Efficiency is evaluated by dividing window averaged power input (voltage × current) by window averaged output power. Optimizations are performed using the method asynchronous parallel pattern search (APPS) [13] to optimize efficiency by varying six device dimensions L_1, L_2, L_4, r_c, r_a, and input voltage. The optimization is performed as follows: Dakota's built in APPS function chooses design points for simulation, these designs are simulated in parallel using the particle-in-cell code ICEPIC, the objective function (efficiency) is evaluated, and APPS chooses new points based off the objective value. The objective function which APPS attempted to maximize was

$$q(\text{efficiency}) = -\log(\frac{\text{efficiency}}{\text{target efficiency}} - 1).$$

This function q achieves a maximum when the device efficiency reaches the target efficiency. The optimization performed here used a target efficiency = 0.35.

The optimization method APPS allows for nonlinear problems that can be approached in a parallel way. The

method is designed for expensive function evaluations and fewer than 50 input variables [13]. The features of the problem at hand are well suited for the use of APPS. Furthermore, APPS is conveniently built into Dakota.

As alluded to in the introduction, fixing the anode-cathode gap while varying other parameters will mitigate changes in operating frequency. The frequency is also dependent on the input voltage, however the dependency is far less sensitive than the anode-cathode gap relationship to frequency. This is confirmed numerically in this paper but also theoretically in [8] by the rough approximation $f \propto V_0^{1/2}/r_{ak}$, where f is the dominant frequency of the coaxial vircator, V_0 is the diode voltage, and r_{ak} is the anode-cathode gap.

The physical dimensions L_1, L_2, L_4, and r_c are chosen for optimization to tune the interaction region to the virtual cathode and the device frequency. The six parameters used in optimization are not varied absolutely, but are scaled based off the initial device described in Section III. The plots showing the convergence of the scales with respect to iteration are in Fig. 4 and 5. The optimization is taken to convergence, that is, the optimization algorithm APPS is designed to exit when the merit function no longer increases with additional iterations. The net result is at least a local maximum in efficiency but possibly a global maximum in efficiency.

V. Discussion of Results

Fig. 4 and Fig. 5 show the convergence of the APPS method. The variables which had the most impact, straying away from their original values, are r_a and r_c. The optimization, after about 200 iterations, converged to a device with the six physical parameters $L_1 = 5.53$, $L_2 = 2.10$, $L_e = 3.20$, $L_3 = 0.64$, $L_4 = 3.02$, $r_a = 4.14$, $r_c = 1.49$, $h = 1.2$, all units in centimeters. With a anode-cathode gap of 2.65 cm, the diode had a voltage and current of 566 kV and 18.4 kA respectively. The resulting source produced an average of 2.08 GW of output power, which is pictured in Fig. 6, operating with frequency 4.43 GHz. The output power is over 98% in the TM_{01} mode. The power conversion efficiency was 20% during stable operation (the time period between 15 and 30ns).

Fig. 4 and Fig. 5 show how the APPS method iterated with respect to each parameter. The variables which had the most impact, straying away from their original values, are r_a and r_c. This is a logical result as these variables directly tune the radial size of the interaction cavity.

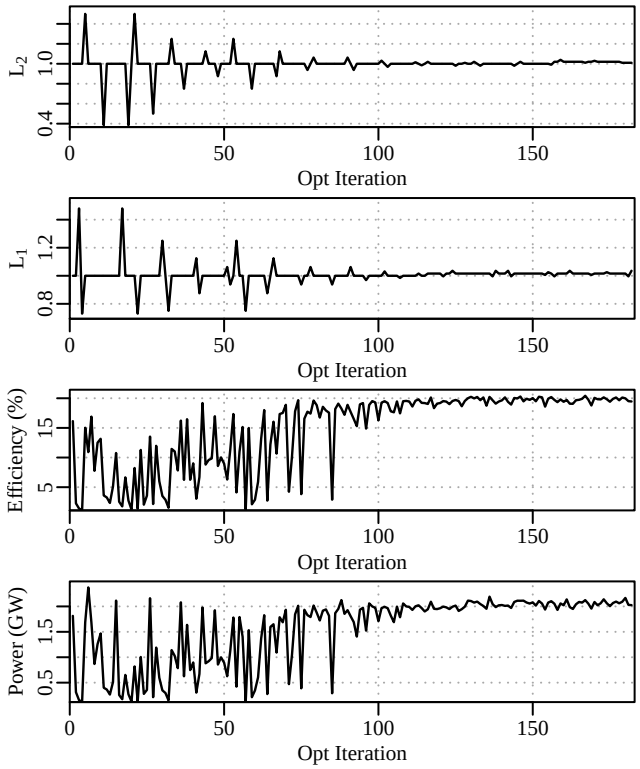

Fig. 5: Plots of optimization iterations converging for Efficiency, Power, and various variable scales.

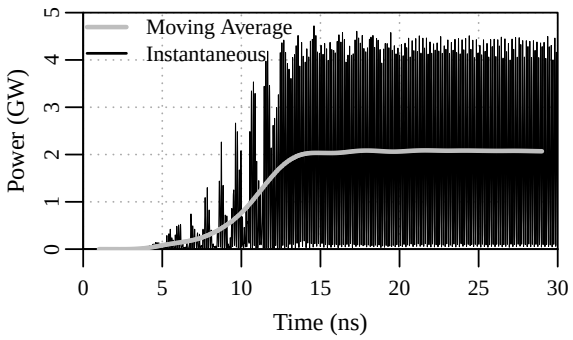

Fig. 6: Instantaneous and averaged output power plot for optimized C-band coaxial vircator.

A. Power Sensitivity to Voltage and Foil Transparency

The optimized nature of this coaxial vircator suggests it is finely tuned to its designed parameters. In a laboratory setting, building this source with precise geometric variables is readily achievable. However, reliably obtaining the correct diode voltage is not always possible. Furthermore, correctly predicting the theoretical transparency of the anode foil is not obvious. Fig. 8 displays the design's output power sensitivity to both foil transparency and input voltage. The voltage plot shows

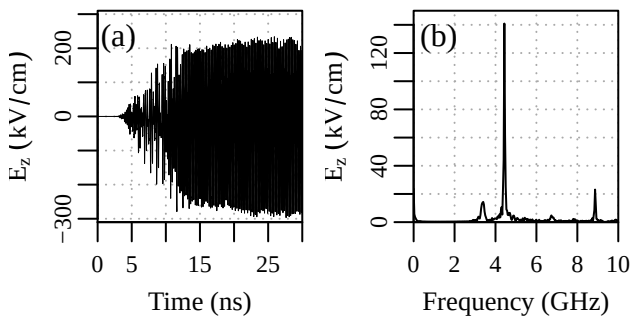

Fig. 7: Plots of downstream electric field (a) and Fourier transform of downstream electric field (b).

that the source is somewhat robust when it comes to voltage, achieving more than 1 GW window-averaged output power for voltages above 500 kV. However, one can notice that the 500 kV diode voltage is a critical point. Incrementally lowering the voltage below 500 kV causes the output power to rapidly drop to near 0.

The device has an abrupt drop in power with a foil transparency below 0.93. Reference [14] shows that a 5 μm anode foil made of copper or aluminum achieves greater than 0.93 transparency in the presence of an electron beam with energy 250 keV or larger. Hence, with the correct choice of anode foil, these results should be available in experiment.

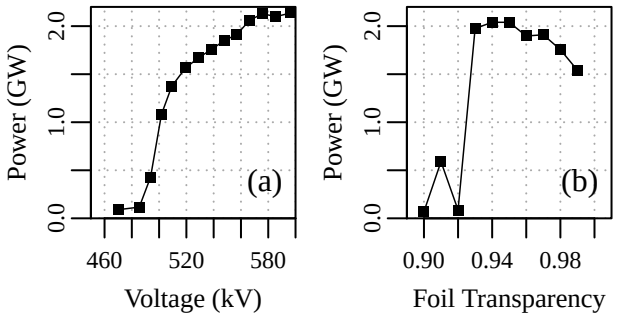

Fig. 8: Plots of coaxial vircator's output power sensitivity (with all other parameters held constant) to (a) input voltage and (b) foil transparency.

B. Cathode Design Considerations

In order to prevent explosive emission in unwanted areas on the cathode, electric field values along the the cathode surface, except for the emission region, are preferred to be below 300 kV/cm. The optimized coaxial vircator has several regions along its cathode where surface E-field exceed 300 kV/cm; these are the sharp corners of the cathode and the region of the cathode directly below the reflecting ring. In order to reduce these fields, the sharp corners of the cathode are rounded and the ring reflector and inner conducting rod are made smaller (h reduced by 10% r_c reduced by 5%).

The modified geometry is pictured in Fig. 9. These adjustments result in a configuration that effectively reduce the E-field strength. Pictured in Fig. 10 are plots of the maximum E-field along the inner and outer cathodes. Without the cathode changes, the maximum E-field strength on the inner cathode rod is 332 kV/cm; 298 kV/cm for the outer cathode. Rounding the cathode and shrinking h and r_c reduce both of the cathodes' E-field strengths below 300 kV/cm. These adjustments, however, come at a cost: the output power is reduced to 1.86 GW and the efficiency to 17.6%. The impedance and frequency are both unchanged.

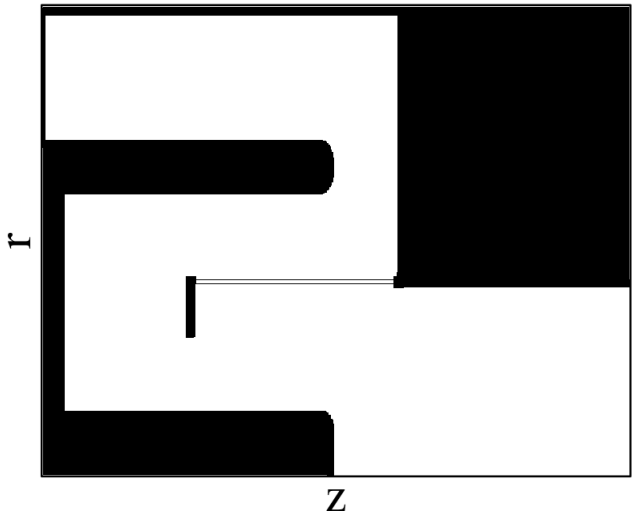

Fig. 9: Modified geometry of coaxial vircator with rounded cathode, reduced inner cathode radius, and smaller reflecting ring.

VI. Conclusion

Presented in this article is a gigawatt class C-band coaxial vircator with an averaged output power efficiency of 20%. Such an efficiency was achieved using a non-gradient parallel optimization method APPS which performed over 200 simulations. The merit function was chosen to maximize efficiency and was run until it converged. Furthermore, the sensitivity of the source to voltage and foil transparency were investigated. It was shown that for diode voltages exceeding 500 kV, the source will operate in a high power regime, but will perform poorly at voltages below 500 kV. It was shown

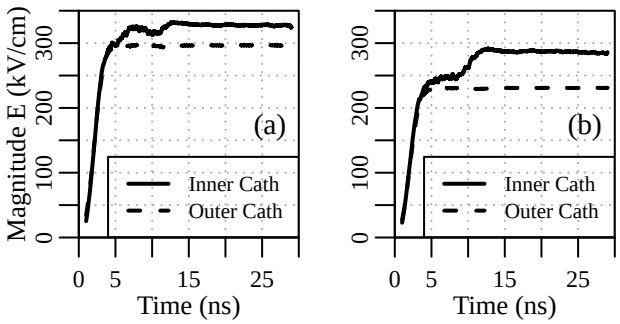

Fig. 10: Plots of maximum E-field values along inner cathode rod and outer cathode. Plot (a) shows these values for the unaltered optimized C-band coaxial vircator. Plot (b) shows these E-field values for the configuration depicted in Fig. 9.

that the device is quite sensitive to foil transparency, however, the foil technology to achieve full performance is available.

Finally, to prevent unwanted explosive emission on the cathode, methods for reducing E-field strength were explored. By reducing the the radius of the inner cathode rod, the size of reflecting ring, and by rounding sharp cathode edges, all cathode E-fields were below 300 kV/cm. The resulting device operated at 4.43 GHz with an average output power of 1.86 GW (17.8 % efficiency).

REFERENCES

[1] R. J. Barker and E. Schamiloglu, *High-power microwave sources and technologies*. IEEE Press, 2013.

[2] J. Benford, J. A. Swegle, and E. Schamiloglu, "Vircators, gyrotrons and electron cyclotron masers, and free-electron lasers," in *High power microwaves*. CRC Press, 2007, ch. 10, pp. 435–500.

[3] S. Champeaux, P. Gouard, R. Cousin, and J. Larour, "3-d pic numerical investigations of a novel concept of multistage axial vircator for enhanced microwave generation," *IEEE Transactions on Plasma Science*, vol. 43, no. 11, pp. 3841–3855, Nov 2015.

[4] Z. Yang, G. Liu, H. Shao, J. Sun, Y. Zhang, H. Ye, and M. Yang, "Numerical simulation study and preliminary experiments of a coaxial vircator with radial dual-cavity premodulation," *IEEE Transactions on Plasma Science*, vol. 41, no. 12, pp. 3604–3610, Dec 2013.

[5] J. J. Ou, H. Shao, Y. C. Zhang, X. Z. Xiong, and C. Liao, "Theoretical analysis and simulation study on a coaxial vircator with enhanced modulation," *Journal of Plasma Physics*, vol. 81, no. 5, p. 905810511, 2015.

[6] W. Yang, Z. Dong, and Y. Dong, "3-d particle-in-cell simulations on a novel high-power and high-efficiency coaxial triode vircator," *IEEE Transactions on Electron Devices*, vol. 63, no. 9, pp. 3713–3718, Sept 2016.

[7] G. Liu, H. Shao, Z. Yang, Z. Song, C. Chen, J. Sun, and Y. Zhang, "Coaxial cavity vircator with enhanced efficiency," *Journal of Plasma Physics*, vol. 74, no. 2, p. 233–244, 2008.

[8] Q. Xing, D. Wang, F. Huang, and J. Deng, "Two-dimensional theoretical analysis of the dominant frequency in the inward-emitting coaxial vircator," *IEEE Transactions on Plasma Science*, vol. 34, no. 3, pp. 584–589, June 2006.

[9] W. Jeon, K. Y. Sung, Y. Jung, J. G. Kim, and E. H. Choi, "A diode design study of the virtual cathode oscillator with ring-type reflector," in *Digest of Technical Papers. PPC-2003. 14th IEEE International Pulsed Power Conference (IEEE Cat. No.03CH37472)*, vol. 2, June 2003, pp. 1143–1146 Vol.2.

[10] B. Adams *et al.*, "Dakota a multilevel parallel object-oriented framework for design optimization parameter estimation uncertainty quantification and sensitivity analysis: Version 6, type = 0 user's manual," Sandia Technical Report SAND2010-2183, Tech. Rep., 2015.

[11] R. E. Peterkin and J. W. Luginsland, "A virtual prototyping environment for directed-energy concepts," *Computing in Science Engineering*, vol. 4, no. 2, pp. 42–49, Mar 2002.

[12] T. Garrett, "Zagorodnov conformal particle in cell simulations," to be submitted.

[13] P. Hough, T. Kolda, and V. Torczon, "Asynchronous parallel pattern search for nonlinear optimization," *SIAM Journal on Scientific Computing*, vol. 23, no. 1, pp. 134–156, 2001. [Online]. Available: https://doi.org/10.1137/S1064827599365823

[14] G. Singh and S. Chaturvedi, "Pic simulation of effect of energy-dependent foil transparency in an axially-extracted vircator," *IEEE Transactions on Plasma Science*, vol. 32, no. 6, pp. 2210–2216, Dec 2004.

DISTRIBUTION LIST

DTIC/OCP
8725 John J. Kingman Rd, Suite 0944
Ft Belvoir, VA 22060-6218 1 cy

AFRL/RVIL
Kirtland AFB, NM 87117-5776 1 cy

Bud Denny
Official Record Copy
AFRL/Effects and Modeling 1 cy